Dual-Band Tunable Screen Using Complementary Split Ring Resonators

B. Sanz-Izquierdo, E. A. Parker, and J. C. Batchelor

The link to this paper on IEEE Xplore® is

http://dx.doi.10.1109/TAP.2010.2072900

The DOI is: 10.1109/TAP.2010.2072900

Dual-Band Tunable Screen Using Complementary Split Ring Resonators

B. Sanz-Izquierdo, E. A. Parker, and J. C. Batchelor

***Abstract*—Active frequency selective surfaces (FSS) based on slot-form split ring resonators are described. Switching and tuning have been achieved using two different biasing circuit configurations. The first design switches ON and OFF the two concentric rings separately, producing four distinct transmission responses. The second design is able to vary the capacitance of the two split rings, allowing independent dual-band frequency tuning. The active FSS incorporate commercially available, low cost, surface mount switched PIN diodes and varactor diodes. The operation of the surfaces covers a wide band frequency range within the UHF spectrum, which is desirable for applications such as the modification of the EM architecture of buildings. Measurements compare well with the simulations.**

***Index Terms*—Electromagnetic wave propagation, EM architecture, frequency selective surfaces, PIN diodes, switching, tuning.**

I. INTRODUCTION

Split ring resonators (SRR) and their complementary slot-form (CSRR) have attracted significant research interest in recent years. In particular, configurations with two concentric split rings oriented 180° relative to each other, are one of the most commonly used structures in metamaterials [1], [2]. Electromagnetic band gap structures (EBG), negative ε, negative μ, and left handed media (LH) are some of the metamaterials where SRR have been employed. The SRR and their Babinet complement (CSRR) are characterized by their compact size compared to their operating wavelength and by a strong magnetic/ electric current near resonance. This feature relates to the large capacitance created between the two rings. An extensive number of devices have been demonstrated using this element, including: filters [3], couplers [4], power divides [5] and antennas [6]. More recently, the application to frequency selective surfaces has been presented [7] and analyzed [8]. The addition of active components to frequency selective surfaces (FSS) have been widely investigated [9]–[14]. Switching [9]–[12] and tuning [13], [14] has been achieved. Switching has typically two states: transmitting and reflective, while tuning offers a smooth modification of the transmission response. Active FSS consisting of metallic dipole patches have been extensively reported [9]–[11], [13], but the development of slot-form active FSS is more recent [12], [14]. In [12], [14], the slot-form of active FSS consists of square loop slots etched on one side of an FR4 substrate, with the biasing circuit on the other side, and metallic vias connecting both sides. A novel technique for slot FSS has been recently proposed by the authors [15]. The technique consists of a double sided structure sandwiching a very thin dielectric substrate. There is no need for metallic vias and the biasing circuit is etched at the rear of the slot FSS.

This communication demonstrates dual band switching, and also tuning, singly polarized frequency selective surfaces using complementary split ring resonators. Two active FSS configurations are presented.

The first switches the two slots individually and the second varies their capacitance. The novel biasing technique described in [15] is used in order to achieve such a level of control over the surfaces. Switching and tuning two resonant modes over a wide band could have applications on the modification of the electromagnetic architecture of buildings [16]–[19]. The studies presented here are mainly experimental.

II. SWITCHABLE SPLIT RING RESONATORS

The transmission response of frequency selective surfaces consisting of split square loops and rings were studied in [20], [21]. One split in the loop produces a resonant frequency at approximately half of the frequency of the full loop. The resulting structure is very stable to angle of incidence, though singly polarized. The behavior of FSS based on two concentric split ring resonators has been recently analyzed [7], [8], [22]. There, they were designed to study the single band response due to the close proximity of the rings. In this communication, the two concentric rings have been arranged to produce a clear dual band-pass response. The active FSS consists of a double-sided structure with the passive slot FSS on one side and the active circuit with the PIN diodes on the other side. A schematic section view of the active FSS technique is shown in Fig. 1(d). The two metallic layers sandwiched a 0.05 mm thick polyester substrate. Fig. 1(b) illustrates a biasing configuration for switching the two split-rings individually. A photograph of the rear of 3×3 elements of the array is shown in Fig. 2(a). 10$\times$10 cells organized in a square with periodicity P = 18 mm were fabricated. The dimensions of the split rings at the front (Fig. 1(a)) were: R = 3.5 mm, a = c = 1 mm and b = 2.5 mm. The lines of the biasing circuit were between 0.5 mm and 1 mm wide. BAR64-02 silicon PIN diodes with forward resistance R_s = 2.1 ohms and capacitance at 0 volts of C_s = 0.2 pF were employed. The capacitance added to the FSS decreased the electric length of the slots from the typical $\lambda/2$ to $\lambda/2.75$, with λ the dimension of the corresponding resonant free-space wavelength. The dimensions of the slots were derived using CST Microwave Studio. Simulations were regarded only as a design guide to experimental implementation and their results are only described for the first design. The very thin dielectric substrate increased significantly the meshing and simulation processes. The diodes were considered as lumped elements with characteristic resistance or capacitance depending whether they were in ON or OFF states. Measurements were carried out using two log periodic antennas at 0.6 m from a 3×3 m absorbing panel containing the FSS. The system was calibrated relative to an open aperture of approximately 190×190 mm in the centre of the panel. The independent switching of the two concentric split rings allowed for four possible states: all diodes switched OFF, all diodes switched ON, diodes on *inner* rings ON and *outer* rings OFF and diodes on *inner* rings OFF and *outer* rings ON. The transmission response with all the diodes in the OFF state and the electric field as in Fig. 1(a) (*y-axis*) is shown in Fig. 3. At normal incidence, the FSS resonated at 2.5 GHz and 5 GHz with insertion losses of 1.1 dB and 2.5 dB respectively. Simulations found that the losses were mainly due to the effect of the biasing circuit and PIN diodes, which also produced the split in the higher band. The FSS was very stable to angle of incidence and transmission levels decreased at the lower band, by 1.0 dB at TM45 and 2.9 dB at TE45.With all the diodes in the ON state (Fig. 4), resonance occurred for a slot length of $\lambda/2$ and 2λ, with the lower band due to the effect of the biasing circuit while the higher band being the one expected from opening loops [19]. Transmission levels were under -15 dB at 2.5 GHz and about -20 dB at 5 GHz.

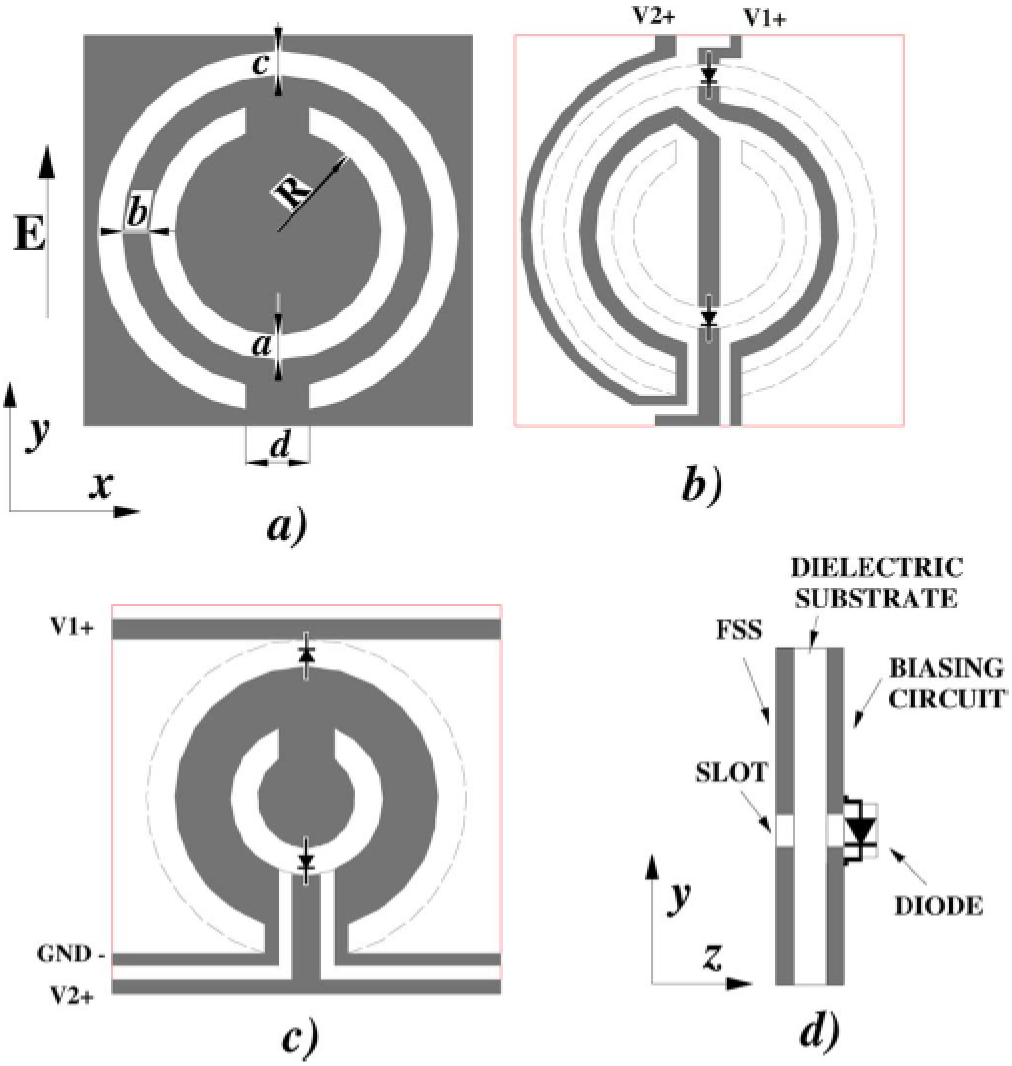

Fig. 1. Active complementary split ring configurations: (a) front view of one unit cell, (b) rear view of the biasing configuration for switching, (c) biasing configuration for tuning, (d) schematic section view of the technique employed.

The transmission response when the diodes on the *inner* rings were in the ON state and the diodes on the *outer* rings in the OFF state is shown in Fig. 5. The resonance at 2.5 GHz did not vary considerably, and its insertion loss was about 1dB at normal incidence, 0.5 dB at TM45 and 4.5 at TE45. At 5 GHz, the FSS was opaque with the transmission levels well below -15 dB.

Fig. 6 shows the transmission response for the diodes on the *outer* rings in the ON state and the diodes on the *inner* rings in the OFF state. At 2.5 GHz, the FSS switched to reflective mode, with transmission levels less than -14 dB. At 5 GHz, transmission levels were -5 dB at normal incidence and -8 dB at TM45 and TE45. The measured transmission response for the electric field parallel to the x- axis did not vary significantly when the diodes were switched ON and OFF. This can be explained by applying Babinet's principle to the FSS described in [19], where transmission did not change for the E field perpendicular to the side cut in the loop due to the sinusoidal distribution of the induced current. Here, the FSS resonated at about 7 GHz, the wavelength of one slot length.

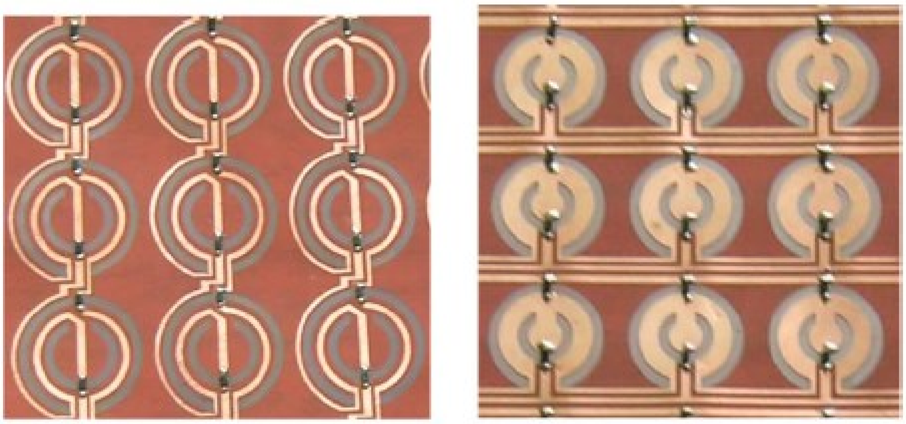

(a) (b)

Fig. 2. Two biasing circuit configurations for CSRR: (a) switching, (b) tuning.

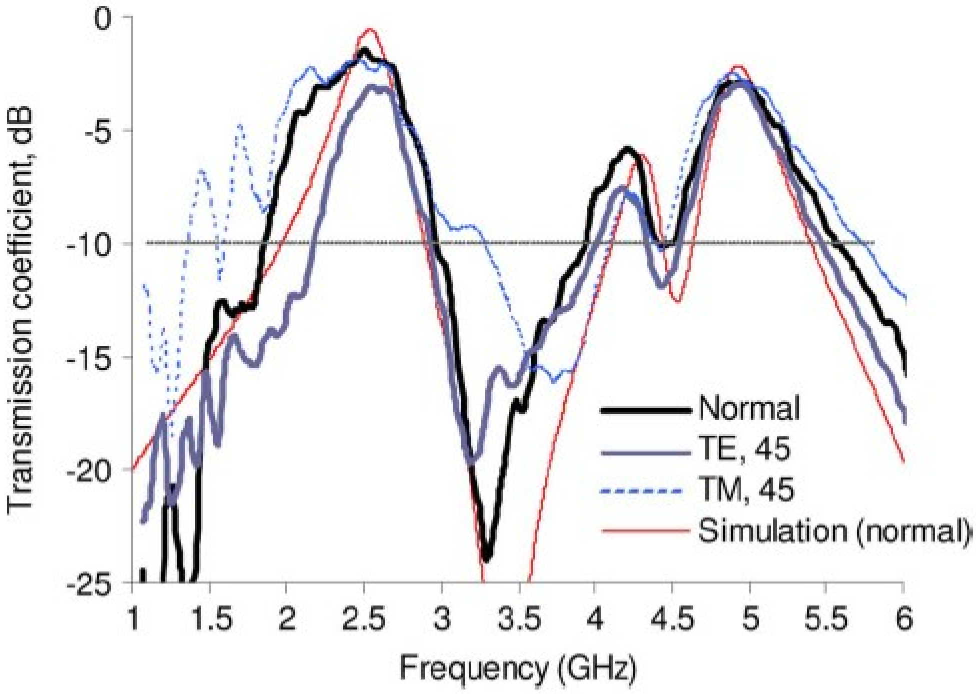

Fig. 3. Measured transmission response with all the diodes in the OFF state.

III. DUAL—BAND TUNABLE SPLIT RING RESONATORS

Dual band *tuning* of split ring resonators was achieved using the biasing circuit configuration in Fig. 1(c). A photograph of the circuit at the rear of 3 × 3 cells is shown in Fig. 2(b). Three lines run along all cells in a row: one centre line is the common ground where the anodes of the varactors connect, one exterior line connects to the cathode of the varactor on the *outer* split ring and another exterior line connects the cathode of the varactor on the *inner* split ring. BB857 silicon varactor diodes with a tunable capacitance range from 0.5 pF (28 V) to 7.2 pF (1 V) were chosen. The FSS itself consisted of a 13 $\times$ 13 array on a rectangular lattice of periodicity P = 14 mm. The main dimensions of the FSS (Fig. 1(a)) were: R = 1.75 mm, a = c = 1 mm, b =2 mm. The widths of the strips providing the bias at the rear were between 0.5 and 2 mm.

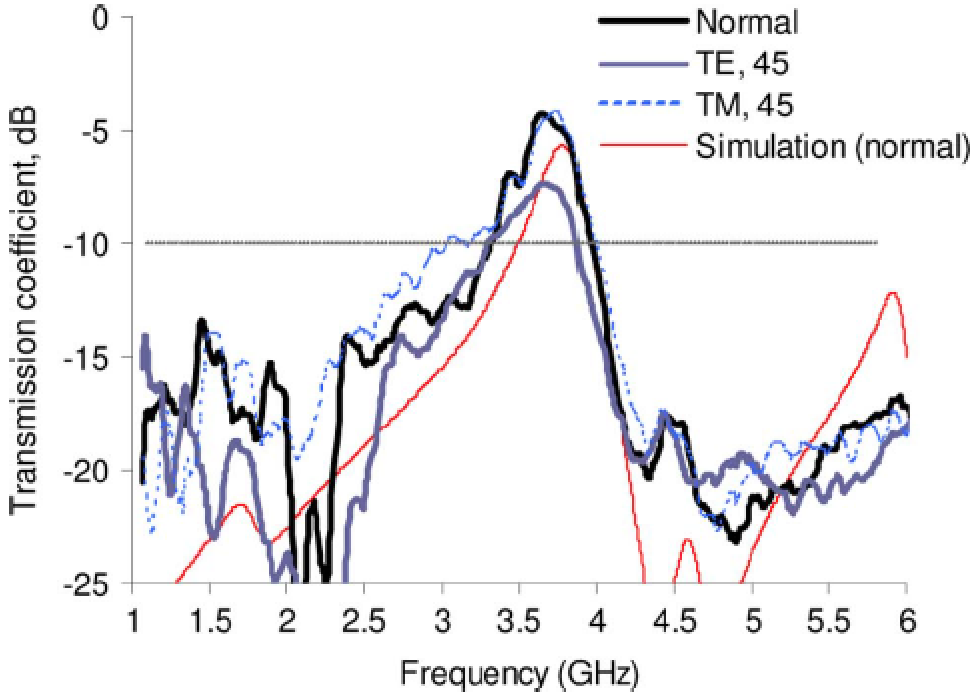

Fig. 4. Measured transmission response with all the diodes in the ON state.

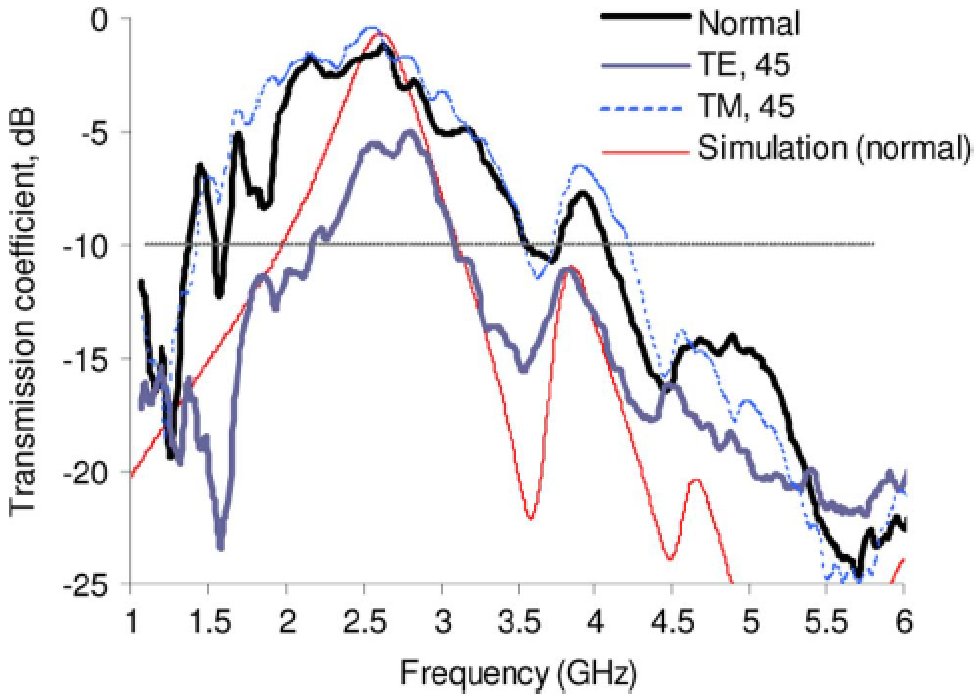

Fig. 5. Measured transmission response with the diodes on the *inner* rings in the ON state and the diodes on the *outer* rings in the OFF state.

The measured transmission response at normal incidence of the tunable FSS for 5, 10, 15, 20 and 28 volts across all the varactors is shown in Fig. 7. At the lower frequency band, the resonant frequency increased from 1.5 GHz for 5 V to 2.6 GHz for 28 V, while the passband insertion loss decreased from 7.2 dB to 1.6 dB. At the higher band, the resonant frequency increased from 2.2 GHz to 4.0 GHz and the insertion loss decreased from 15 dB to 5.4 dB. The measured transmission response of the tunable FSS when a constant voltage of 28 V is applied to the varactor on the *inner* ring and the voltage across the varactor on the *outer* ring is varied between 5 and 28 volts is shown in Fig. 8. The lowest resonant frequency increased again from 1.5 GHz for 5 V to 2.6 GHz for 28 V and the passband insertion loss decreased from 7 dB to 1.6 dB. The resonant frequency of the higher band remained constant at 4 GHz but its insertion loss decreased from 9.5 dB to 5.4 dB.

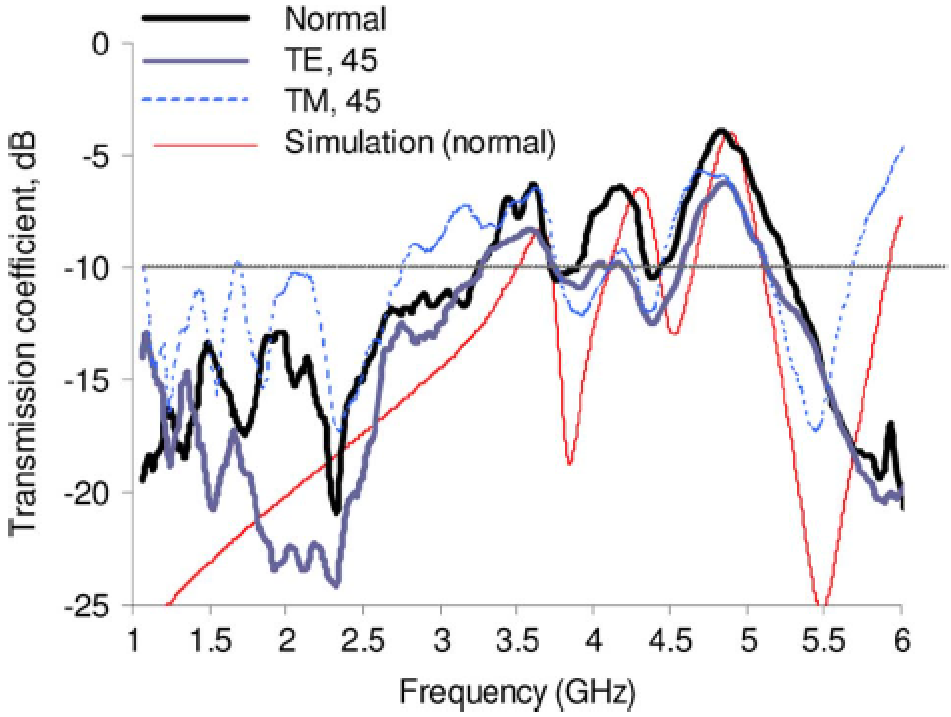

Fig. 6. Measured transmission response with the diodes on the *inner* rings in OFF state and the diodes on the *outer* rings in the ON state.

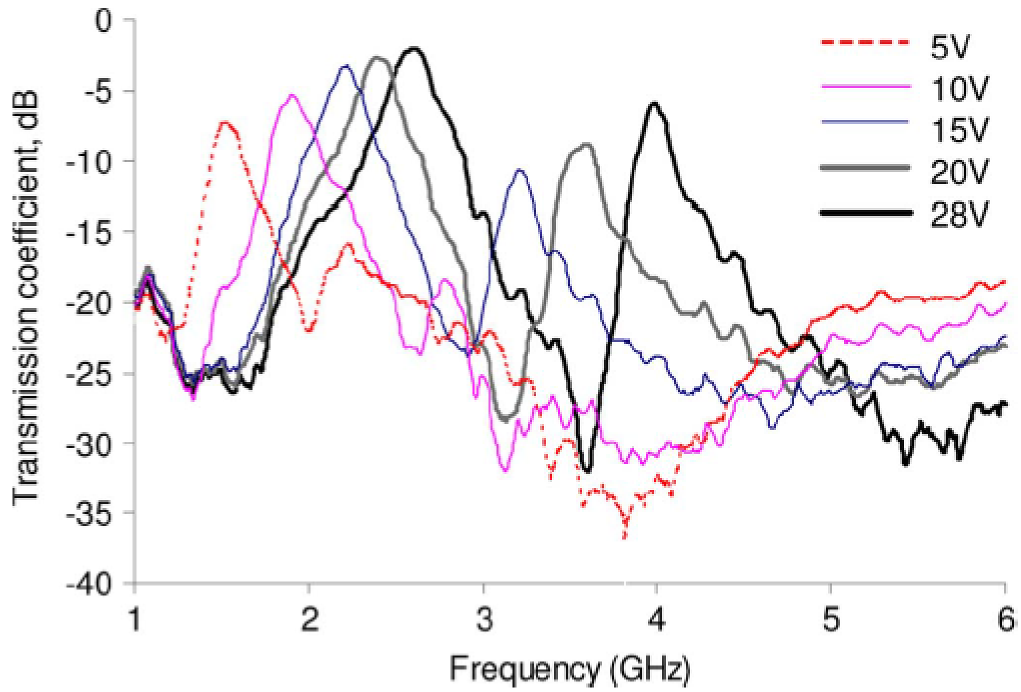

Fig. 7. Measured transmission response at normal incidence for simultaneous tuning of both split rings.

Fig. 9 shows the measured transmission response at normal incidence for a constant voltage of 28 V across the varactor on the *outer* ring and varying the voltage of the varactor on the *inner* ring between 5 V and 28 V. The resonant frequency of the lower band remained constant at 2.6 GHz except for 10 V biasing when the proximity of the second mode slightly split the peak. The higher band, however, is not present at 5V and increases from 2.8 GHz for 10V to 4.0 GHz for 28 V. The result is remarkable and shows that the control of the higher band is limited by the resonant frequency of the lower band. To verify this, a similar experiment was carried out where the voltage on the varactor on the *outer* ring was fixed to 10 V and the voltage in the *inner* ring was varied. On this occasion, the lower frequency resonates at 1.9 GHz and the higher frequency transmission band exists at about 2.2 GHz for an *inner* ring bias of 5 V. As in the previous configuration, the transmission response for the electric field parallel to the x- axis did not vary significantly when the voltage across the varactors was modified.

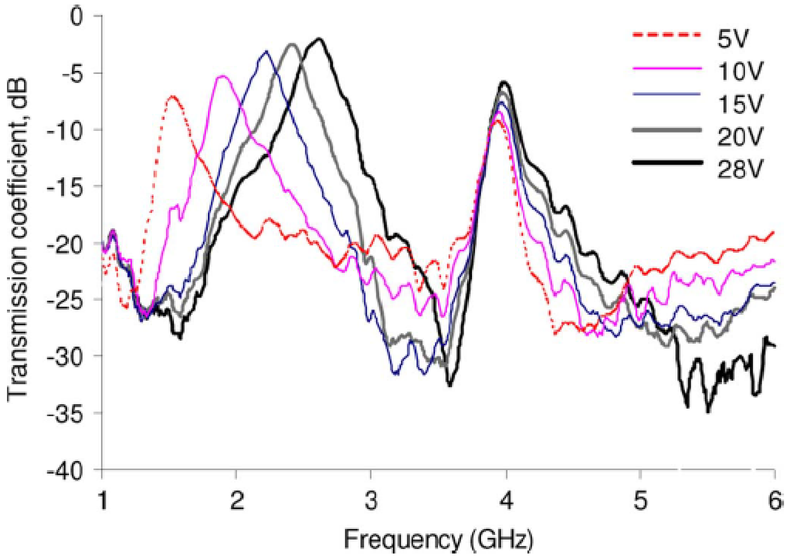

Fig. 8. Measured transmission response at normal incidence for a constant voltage of 28 V across the varactor on the *inner* ring and varying the voltage of the varactor on the *outer* ring.

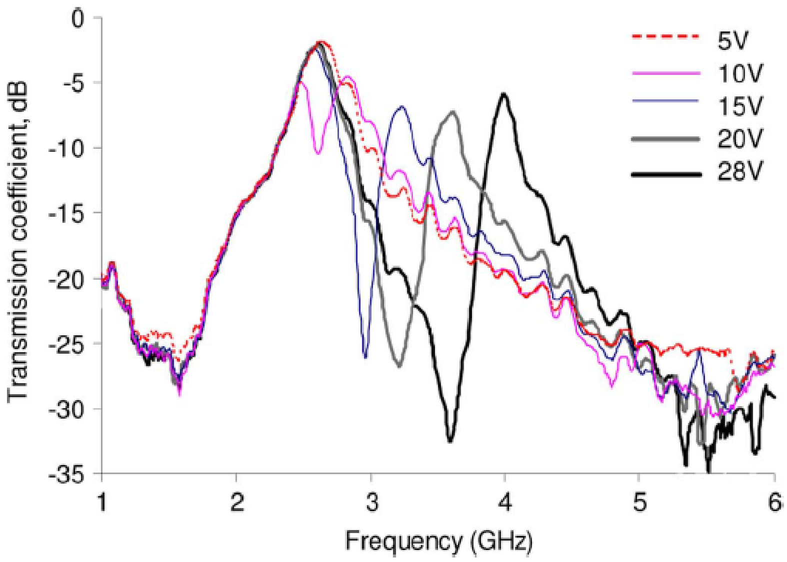

Fig. 9. Measured transmission response at normal incidence for a constant voltage of 28 V across the varactor on the outer ring and varying the voltage of the varactor on the inner ring.

IV. CONCLUSION

Active frequency selective surfaces using complementary split ring resonators (CSRSS) have been presented. The FSS uses a recently developed technique where a very thin substrate avoids the need for metallic vias in active frequency selective slots. Dual-band switching and tuning has been demonstrated using two different biasing configurations. In the first configuration, a 4-stage switching FSS was achieved by biasing the two concentric split rings through different bias lines. In the second, independent tuning over the two resonant modes created by the concentric rings, giving inner and outer tunable frequency ranges of about 55% for bias voltages between 5 V and 28V. One application is in the general field of dynamic modification of the EM Architecture of the built environment. The technique employed for the active FSS has been filed as Tunable Surface filing no. GB0902380.6

ACKNOWLEDGMENT

The authors would like to thank S. Jakes for assisting in the fabrication of the FSS.

REFERENCES

[1] J. B. Pendry, A. J. Holden, D. J. Robbins, and W. J. Stewart, “Magnetism from conductors and enhanced nonlinear phenomena,” *IEEE Trans. Microw. Theory Tech.*, vol. 47, pp. 2075–2084, 1999.

[2] D. R. Smith, W. J. Padilla, D. C. Vier, S. C. Nemat-Nasser, and S. Schultz, “Composite medium with simultaneously negative permeability and permittivity,” *Phys. Rev. Lett.*, vol. 84, pp. 4184–4187, May 2000.

[3] W. Menzel, L. Zhu, K.Wu, and F. Bogeslack, “On the design of novel compact broad-band planar filters,” *IEEE Trans. Microw. Theory Tech.*, vol. 51, no. 2, pp. 364–370, Feb. 2003.

[4] G. Siso, J. Bonache, M. Gil, J. Garcia-Garcia, and F. Martin, “Compact rat-race hybrid coupler implemented through artificial left handed and right handed lines,” in *IEEE MTT-S Int. Microw. Symp. Dig.*, Honolulu, HI, June 2007, pp. 25–28.

[5] M. Gil, J. Bonache, I. Gil, J. Garcia-Garcia, and F. Martin, “Miniaturization of planar microwave circuits by using resonant-type left handed transmission lines,” *IET Microw. Antennas Propag.*, vol. 1, pp. 73–79, Feb. 2007.

[6] H. Zhang, Y.-Q. Li, X. Chen, Y.-Q. Fu, and N.-C. Yuan, “Design of circular/dual-frequency linear polarization antennas based on the anisotropic complementary split ring resonator,” *IEEE Trans. Antennas Propag.*, vol. 57, pp. 2572–2581, Oct. 2009.

[7] M. Beruete, R. Marques, J. D. Baena, and M. Sorolla, “Resonance and cross-polarization effects in conventional and complementary split ring resonators periodic screens,” in *IEEE Antennas Propag. Soc. Int. Symp.*, Washington, DC, Jul. 2005, vol. 3–8, pp. 794–797.

[8] R. Marques, J. D. Baena, M. Beruete, F. Falcone, T. Lopetegi, M. Sorolla, F. Martin, and J. Garcia, “Ab initio analysis of frequency selective surfaces based on conventional and complementary split ring resonators,” *J. Opt. A: Pure Appl. Opt.*, no. 7, pp. S38–S43, 2005.

[9] T. K. Chang, R. J. Langley, and E. A. Parker, “Active frequency selective surfaces,” *IEE Proc., Part H*, vol. 143, pp. 62–66, 1996.

[10] A. Tenant and B. Chambers, “Experimental dual polarized phase-switched screen,” *Electron. Lett.*, vol. 39, no. 1, pp. 119–121, Jan. 2003.

[11] B. M. Cahill and E. A. Parker, “Field switching in an enclosure with active FSS screen,” *Electron. Lett.*, vol. 37, no. 4, 15, pp. 244–245, Feb. 2001.

[12] G. I. Kiani, K. L. Ford, L. G. Olsson, K. P. Esselle, and C. J. Panagamuwa, "Switchable frequency selective surface for reconfigurable electromagnetic architecture of buildings," *IEEE Trans. Antennas Propag.*, vol. 58, no. 2, Feb. 2010.

[13] A. Tennant and B. Chambers, "A single-layer tuneable microwave absorber using an active FSS," *IEEE Microw. Wireless Compon. Lett.*, vol. 14, no. 1, pp. 46–47, Jan. 2004.

[14] C. Mias and C. Tsakonas, "Waveguide demonstration of varactor-diode-tunable band-pass frequency selective surfaces," *Microw. Opt. Technol. Lett.*, vol. 45, 1, pp. 62–66, Feb. 25, 2005.

[15] B. Sanz-Izquierdo, E. A. Parker, J. B. Robertson, and J. C. Batchelor, "Tuning technique for active FSS arrays," *Electron. Lett.*, vol. 45, no. 22, pp. 1107–1109, Oct. 22, 2009.

[16] M. Hook and K. Ward, "A project to demonstrate the ability of frequency selective surfaces and structures to enhance the spectral efficiency of radio systems when used within buildings," 2004, Ofcom ref. AY4462A.

[17] E. A. Parker and S. Massey, "Application of FSS structures to selective control the propagation of signals into and out of buildings," [Online]. Available: http://www.ofcom.org.uk/research/technology/spectrum_efficiency_scheme/ses2003-04/ay4464a/survey.pdf Aug. 2009, Ofcom ref AY4464A, Annex 5: "Survey of Active FSS", 2004

[18] E. A. Parker, J. B. Robertson, B. S. Izquierdo, and J. C. Batchelor, "Minimal size FSS for long wavelength operation," *Electron. Lett.*, vol. 44, no. 6, pp. 394–395, Mar. 2008, (2008);.

[19] B. Sanz-Izquierdo, I. T. Ekpo, J.-B. Robertson, E. A. Parker, and J. C. Batchelor, "Wideband EM architecture of buildings: Six-to-one dualpassband filter for indoor wireless environments," *Electron. Lett.*, vol.44, no. 21, pp. 1268–1269, 2008.

[20] A. D. Chuprin, E. A. Parker, and J. C. Batchelor, "Resonant frequencies of open and closed loop FSS arrays," *Electron. Lett.*, vol. 36, no. 19, pp. 1601–1603, Sept. 2000.

[21] A. E. Martynuk, A. E. , and J. I. Martinez Lopez, “Frequency selective surfaces based on shorted ring slots,” *Electron. Lett.*, vol. 37, pp. 268–269, 2001.

[22] R. Dickie, R. Cahill, H. S. Gamble, V. F. Fusco, P. G. Huggard, B. Moyna, M. Oldfield, N. Grant, and P. de Maagt, “Polarisation independent bandpass FSS,” *Electron. Lett.*, vol. 43, pp. 1013–1015, 2007.